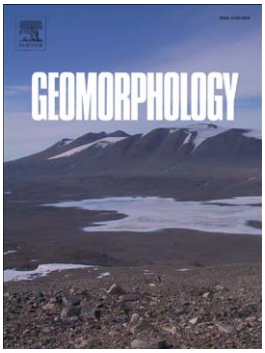

Simulating reef response to sea-level rise at Lizard Island: A geospatial approach

S.M. Hamylton, J.X. Leon, M.I. Saunders, C.D. Woodroffe

PII: S0169-555X(14)00118-4
DOI: doi: 10.1016/j.geomorph.2014.03.006
Reference: GEOMOR 4684

To appear in: *Geomorphology*

Received date: 9 October 2012
Revised date: 24 September 2013
Accepted date: 2 March 2014

Please cite this article as: Hamylton, S.M., Leon, J.X., Saunders, M.I., Woodroffe, C.D., Simulating reef response to sea-level rise at Lizard Island: A geospatial approach, *Geomorphology* (2014), doi: 10.1016/j.geomorph.2014.03.006

Simulating reef response to sea-level rise at Lizard Island: a geospatial approach

S.M. Hamylton[1], J.X. Leon[1,2], M. I. Saunders[2] and C.D. Woodroffe[1]

School of Earth and Environmental Sciences, University of Wollongong, Wollongong, New South Wales 2522, Australia

Global Change Institute, University of Queensland, Brisbane, Queensland, 4072, Australia

Email: shamylto@uow.edu.au

Tel: +61 02 42213589

Abstract

Sea-level rise will result in changes in water depth over coral reefs, which will influence reef platform growth as a result of carbonate production and accretion. This study simulates the pattern of reef response on the reefs around Lizard Island in the northern Great Barrier Reef. Two sea-level rise scenarios are considered to capture the range of likely projections: 0.5 m and 1.2 m above 1990 levels by 2100. Reef topography has been established through extensive bathymetric profiling, together with available data, including LiDAR, single beam bathymetry, multibeam swath bathymetry, LADS and digitized chart data. The reef benthic cover around Lizard Island has been classified using a high resolution WorldView-2 satellite image, which is calibrated and validated against a ground referencing dataset of 364 underwater video records of the reef benthic character. Accretion rates are parameterised using published hydrochemical measurements taken in-situ and rules are applied using Boolean logic to incorporate geomorphological transitions associated with different depth ranges, such as recolonisation of the reef flat when it becomes inundated as sea level rises. Simulations indicate a variable platform response to the different sea-level rise scenarios. For the 0.5 m rise, the shallower reef flats are gradually colonised by corals, enabling this active geomorphological zone to keep up with the lower rate of rise while the other sand dominated areas get progressively deeper. In the 1.2 m scenario, a similar pattern is evident for the first 30 years of rise, beyond which the whole reef platform begins to slowly drown. To provide insight on reef response to sea-level rise in other areas, simulation results of four different reef settings are discussed and compared at the southeast reef flat (barrier reef), Coconut Beach (fringing reef), Watson's Bay (leeward bay with coral patches) and Mangrove Beach (sheltered lagoonal embayment). The reef sites appear to accrete upwards at a rate commensurate with the rate of rise, thereby maintaining their original profile and position relative to the sea surface and the leeward and lagoonal sites with a low accretion rate maintain a similar profile but slowly gain depth relative to sea-level. The result of this variable response is that elevated features of the reef platform, such as reef patches and crests tend to become more pronounced.

Calcification, reef accretion, Great Barrier Reef, sea-level rise

Introduction

Coral reefs appear particularly vulnerable to climate change. Increases of sea-surface temperature have been shown to result in bleaching of corals (Hughes et al., 2003), and there are concerns that ocean acidification may have already led to a decrease in coral calcification rates (Silverman et al. 2007; De'ath et al., 2009). One of the most certain consequences of global warming is sea-level rise. Reefs appear relatively resilient to a rise in sea level because corals are almost entirely subtidal and are able to accrete vertically. It has even been suggested that the reef flats of many Indo-Pacific reefs, which are emergent at low tide and therefore presently unsuitable for coral establishment, may be recolonised by corals under a higher sea level resulting in a more productive reef community (Hopley et al., 2007; Scopélitis et al. 2011). However, the resilience of reefs in relation to sea-level rise will depend strongly on the rate of rise. Gross morphological change in reef shape over time is dependent on four key properties of the reef platform: *i.* the time of initiation of reef growth, *ii.* the shape and depth of the surface from which the reef grew, *iii.* the rate of reef growth, and *iv.* the relationship between reef growth and sea-level change (Kinsey and Davies, 1975).

The processes of production, breakdown and transport of carbonate result in accumulation and eventual lithification of the reef platforms that comprise the Great Barrier Reef (GBR). A proportion of the carbonate produced does not remain *in situ*, but contributes to the sediments which accumulate in lagoons and which form reef islands. Reef islands appear particularly vulnerable in the face of sea-level rise and many of the villages on the rim of atolls, or on sand cays such as those in central Torres Strait, lie 1 - 2 m above sea level, protected by only a slightly higher beach ridge (Woodroffe, 2008). It has been suggested that rising sea levels will enhance the sedimentary processes underpinning reef-island formation by renewing coral growth on reef flats presently exposed at low tide and unsuitable for coral establishment, and enhancing the transport and reworking of unconsolidated sediment across these reef flats

towards island beaches (Hopley, 1997). By contrast, coral mortality on fringing reefs around granitic islands in the Seychelles has been inferred to reduce their efficacy for shoreline protection, resulting in increased wave erosion of beaches (Sheppard et al., 2005). Although these viewpoints differ in terms of the immediate accretionary or erosional dynamics of reef islands, such studies indicate the significance of the response of the reef itself to sea-level change, and imply that there are critical thresholds in response of reef accretion to the rate of sea-level rise, beyond which abrupt change in both reef platform accretion and island deposition seems inevitable (Hopley 1997; Woodroffe, 2007).

The response of reefs to past changes in sea level provides important insights into how they may respond in future. The history of reef development has been determined from dated cores for many reef platforms on the GBR (summarised in Hopley et al., 2007). Stratigraphical and radiometric-dating studies of reefs have provided evidence of past periods of postglacial sea-level rise during which reefs flourished, as well as periods of very rapid rise, associated with meltwater pulses, during which reefs were drowned or backstepped (Hubbard, 1997; Blanchon et al., 2009). Modern reefs have developed during the past few millennia, in many cases re-establishing over a reefal substrate inherited from a previous sea-level highstand (the last interglacial or a previous interglacial). The pattern of reef growth has varied geographically but has shown one of several responses to sea-level change. In some places, particularly on Caribbean reefs dominated by fast-growing branching corals, it has been possible for reefs to *keep-up* with sea-level rise (Neumann and Macintyre, 1985). Many Indo-Pacific reefs show *catch-up* growth; sea level reached present level about 6000 years ago in this region, but reefs growing from water depths of 10-20 m lagged behind, and caught up with sea level after 6000 yr BP (Davies and Montaggioni, 1985). Several reefs in deeper water were drowned, and have been termed *give-up*. In many parts of the Indo-Pacific region sea level has fallen slightly since a mid-Holocene highstand, an isostatic adjustment related to the

collapse of forebulge regions around the margin of former ice sheets, termed ocean siphoning (Mitrovica and Milne, 2002). Consequently, many reef platforms from these regions have upper reef flat surfaces above the limit to which corals can grow, and which have also '*given up*' because they are exposed at the lowest tides (Dickinson, 2004). The upper limit to coral growth is indicated by the presence of distinctive massive *Porites* corals on reef flats, known as microatolls. The response of fossil and living microatolls (Stoddart et al., 1978) also provides insights into coral growth close to the limiting upper level of mean low water springs (MLWS). These are large discoid corals whose upper surface is dead because they have grown to this limiting water level and which continue to live around their perimeter with lateral growth of 10-20 mm yr^{-1} (Smithers and Woodroffe, 2001).

In contrast to the relative stability of sea level over the past few thousand years, there is now convincing evidence that the sea is rising, partly as a consequence of thermal expansion of ocean waters but also because of the addition of water to the oceans from the melting of continental ice sheets (Church and White, 2006; Rahmstorf, 2007a; IPCC 2007). Global observations of recent sea-level rise based on tide gauge evidence for the past few decades indicate a mean rate of rise of about 1.8 mm yr^{-1} (Church and White 2006). Satellite altimetry, available since the 1990s, indicates that the rate of rise may now be as much as 3.3 ± 0.4 mm yr^{-1} (Rahmstorf et al., 2007b). Climate modelling has produced projections of future sea-level rise that lie between 0.18 and 0.59 m above its 1990 level by 2100 (IPCC, 2007). Several researchers have indicated projections that are higher than these, for example a range of 0.5-1.2 m by 2100 has been suggested (Rahmstorf, 2007), whereas a rise of as much as 2 m by 2100 cannot be entirely discounted (Nicholls et al., 2011).

Increasing water depths over coral reefs will clearly have implications for their suitability for, and rate of, coral growth. Topography is a fundamental control on reef growth, which is the

aggregate of generations of many reef organisms that accrete over geological timescales (spanning from decades to millennia), and water depth is one of the primary constraints on calcification processes in reef communities (Done, 2011). Reef growth is the outcome of net accretion through the precipitation of calcium carbonate from seawater by scleractinian corals and associated organisms, such as coralline algae, green calcified algae, molluscs and benthic foraminifera. Despite many erosional processes that reduce the accumulation of carbonate, reefs gradually consolidate into a three-dimensional structure (Montaggioni and Braithwaite, 2009). Although individual corals can grow at rates of 10 mm yr^{-1} to 100 mm yr^{-1}, reef platform growth occurs more slowly, in the range 1-10 mm yr^{-1}. (Buddemeier and Smith, 1988; Dullo, 2005).

The objective of the present study is to simulate reef platform response to sea-level rise by incorporating available information into a geospatial framework. We present a detailed synthesis of bathymetric data from Lizard Island in the northern Great Barrier Reef that provides the topographic foundation for simulation. Lizard Island was the site of some of the earliest determinations of calcification rates that have been updated over the last forty years, providing site-specific process datasets on the range of rates of carbonate production. A classification of the benthic cover of the reefs around the island has been derived from a high resolution WorldView-2 satellite image, which is calibrated and validated using video records. The model simulates the vertical accretion of reefs at Lizard Island in response to anticipated sea-level trends over the twenty-first century. The spatial variation in benthic communities and their associated carbonate production capacities is captured from the high resolution World-View2 satellite image. Upward reef accretion, given anticipated rates of sea-level rise, is simulated through decadal increments onto a high resolution digital terrain model of the reef platform. The focus of this study is the carbonate that remains *in-situ* and becomes consolidated into the reef platform to make a contribution toward the three-dimensional reef

structure. Carbonate produced by the reef community that is dissolved, bioeroded, transported as sediment to another part of the reef system (contributing to the island beaches or deposited in the lagoon), or exported off the reef platform altogether is not considered.

Two scenarios have been selected for the sea-level rise simulations; these are 0.5 m and 1.2 m above 1990 sea level by 2100. These were chosen to represent respectively the upper rate of the IPCC A1F1 projections of 0.26 – 0.59 m (at 2090-2099 relative to 1980 – 1999) and the empirical projections of sea-level rise of 0.5-1.2 m above 1990 levels being projected by 2100 (Rahmstorf, 2007b). These patterns of sea-level rise are comparable with rates employed by past modelling exercises (Hopley, 1997), which have concluded that reefs will either keep up with sea-level rise (0.5 m by 2100), or become inundated (1.8 m by 2100). This study expands the methodology proposed by Hopley (1997) to a synoptic model that covers the complete reef platform and captures smaller scale variation in benthic community composition. The overall simulation period runs from 2011, when much of the data for the digital terrain model were collected, until 2100.

Study Site

Lizard Island is a granitic island located approximately 30km off the northern Queensland coastline (Fig. 1). The Lizard Island group is composed of three late Permian granite islands: Lizard Island that rises to a height of approximately 395 m above present sea level, and the smaller Palfrey and South Islands to the south. A complex of reefs has developed around these foundations during the Holocene (Rees et al., 2006). A narrow fringing reef occurs around much of the main island, but a broader barrier reef occurs between Palfrey and South Island, and a similar barrier reef extends north from South Island to Bird Island (a minor outcrop of granite on the windward reef flat that lies just south of the main passage into the lagoon). These reefs enclose a lagoon that is up to 10 m deep with a 90m wide channel on the north

eastern side, which experiences fast currents throughout the tidal cycle. The tidal range at Lizard Island is 3 m (Daly, 2005).

The winds blow predominantly from the southeast for approximately 55% of the time and reach speeds of up to 30 ms^{-1} with a secondary northwest component for approximately 25% of the time reaching speeds of 20 ms^{-1}. In turn, these have given rise to transitions in benthic ecological character from reef crest to reef flat in response to spatio temporal variation in water motion, for example, the loss of 95% of incident wave height across the first 50 m of reef encountered on the southeastern facing reef (Madin et al., 2006). The reefs in only a few places on the windward margin appear to have grown up to the limiting MLWS beyond which coral cannot accrete. The reef flats at Lizard Island are generally covered with living coral over much of their upper extent and there are many domed corals whose upper surfaces show no evidence of periodic exposure, indicating that most of the reefs around the island have not reached the upper limit of their growth. Microatolls, colonies of intertidal corals that have reached that limit, are relatively rare, although they occur on the prominent reef flat in front of Coconut Beach, and in places on the southern reef flat. On those reef flats there is presently limited accommodation space with suitable water depths into which coral can grow upward, but the majority of reefs around the rest of the island are not yet limited by accommodation space. For example, the reef flats on either side of South Island have their broad upper surfaces in slightly deeper water and most corals there are continuing to grow vertically.

Lizard Island was chosen for this simulation because of considerable preliminary data on carbonate production rates, including accretion and bioerosion. Rates of carbonate production have been independently determined from the study of water flux and its geochemistry across benthic covers at Lizard Island (LIMER, 1975; Smith and Kinsey, 1976; Smith and Wiebe, 1977; Chisholm, 2000). Measurements of carbonate production observed at Lizard Island are

summarised in Table 1. They range from 1 – 10.3 kg m^{-2} yr^{-1} and appear to be in broad agreement with each other, and comparable to similar results obtained from carbonate production studies elsewhere. These appear to converge around a set of standard values (Kinsey, 1985; Hopley et al., 2007) and are consistent with values derived from census-based methods (Chave et al., 1972). There has also been a preliminary investigation of Holocene reef growth on the windward reef, with three cores recovered that enable an insight into past reef development at this site (Rees et al., 2006). For the purpose of this study, transects across typical reef profiles were established for a detailed assessment of sea-level rise at the Southeast reef flat, Coconut Beach, Watson's Bay and Mangrove Beach. These locations were selected as they represent a range of environmental settings typical of this and other reef platforms across the GBR, including barrier reef (Southeast reef flat) fringing reef (Coconut Beach), leeward bay with coral patches (Watson's Bay) and sheltered lagoonal embayment (Mangrove Beach).

Methodology

Fieldwork

Construction of the Digital Terrain model

A detailed description of the construction of the digital terrain model can be found in Leon et al. (2013). A digital terrain model for Lizard Island was generated by incorporating multiple datasets into a seamless, high spatial resolution (2 m) grid. Datasets included field-collected GPS elevation points, LiDAR, LADSII, single and multibeam bathymtetric points, nautical chart data and empirically derived bathymetry estimations from optical remote sensing imagery (for details, see Table 1 in Leon et al., 2013). *In-situ* bathymetric surveys were carried out using a Ceeducer Pro single beam echosounder mounted to the boat hull in order to determine water depth and derive reef topography. Bathymetric data were corrected for the mounting height of the transducer and tidal fluctuations using readings taken from a tide

gauge that was operated during the collection period. To generate a spatially continuous model of shallow water depth (< 20 m) over the Lizard Island reef system (Fig. 2), a combination of spatial interpolation and regression models known as Regression-Kriging (Hengl et al., 2008) was applied to WV2 wavebands 1 and 3.

The shallow water bathymetric model was combined with a deep water (> 20 m) bathymetric model derived from a series of multi-beam, single-beam and Australian Hydrographic Office charts provided by Geoscience Australia. The complete bathymetric model was combined with LiDAR topographic elevation data acquired as part of the 2009 North Queensland LiDAR capture project. The resulting 4 million points dataset was interpolated using the natural neighbours algorithm (Coleman et al., 2011) to a 2 m spatial resolution seamless digital terrain model (Fig. 2).

Classification of the satellite imagery into benthic cover types

In order to generate a digital representation of benthic cover types, a supervised classification was performed on a WorldView 2 satellite image acquired over Lizard Island on the 10th October 2011 when the water level was at approximately mean sea level. The image classification was calibrated and validated by a field dataset that was collected *in-situ* from December 7th-17th, 2011.

In-situ verification of the satellite imagery

To verify the satellite image *in-situ* and support the census-based parameterisation, three hundred and sixty four snapshots of oblique underwater video footage were collected from a boat over a wide range of reef system types at Lizard Island. Fugawi(TM) navigational software was used to locate the boat in real-time across the satellite image and points of interest were identified, where benthic features or changes in image reflectance were apparent. At each point of interest, an underwater video camera was lowered on a cable from the boat

and held so that it drifted above the sea floor to record for 30 seconds. The geographical position of each verification point was recorded with a GPS. Rapid camera deployment permitted efficient sampling of the benthic community over the large area (approximately 20km^2) of the reef system using 364 records of video footage (Fig. 1).

Image classification

Pre-processing procedures were undertaken to remove the influence of the atmosphere and water column on the image prior to the application of the classification algorithm. For the atmospheric correction, the MODTRAN3 algorithm within the Fast Line-of-site Atmospheric Analysis of Spectral Hypercubes (FLAASH) module was parameterised with image metadata (Cooley et al., 2002). To correct for the influence of the water column, it was necessary to retrieve benthic albedo from the output of the FLAASH module, which represented reflectance at the water surface, R_w, and was a composite of signal from the seafloor and the overlying water column (Equation 1):

$$R_w = (A_b - R_\infty)\, e^{-gz} + R_\infty \qquad \text{Equation 1}$$

Where R_∞ = deep water reflectance (Wm^{-2}sr^{-1})

g = attenuation coefficient (m^{-1}).

z = water depth (m).

A_b = benthic albedo

To implement the correction, it was necessary to decompose the portions of the reflectance signal for which the benthic substrate type and the water column were responsible by calculating the attenuation coefficient. To do so, the average reflectance of 150 pixels selected over deep water was exported for each band and the attenuation coefficient was derived from the gradient of a reflectance plot for pure sand pixels across a depth range (1 – 23 m).

A supervised classification was performed using a maximum likelihood parametric rule on the atmospheric and water-column corrected bands of the Lizard Island reef image. Of the three hundred and sixty four video records collected, fifty were used to define training areas in order to supervise the image classification. The classified output was a digital representation of benthic cover, the content of which was subsequently interpreted with respect to the ground referencing dataset from the video footage records. Each class in the output map was highlighted in turn so that its spatial distribution throughout the reef system could be visually examined. The video footage records falling inside the spatial extent of this class were then extracted from the field dataset and viewed to facilitate interpretation of the classification output and produce a final map of 10 benthic cover classes that were statistically distinct from the video records (Table 2). The overall accuracy of the map produced was validated against an independent set of video records (Congalton, 1991).

Modelling reef accretion for sea-level scenarios from 2011-2100

Parameterisation of reef accretion

To generate a synoptic model of reef accretion that encompassed the complete reef system, published data were used directly to model platform evolution (Table 1). In some instances it was necessary to employ accretion rates for reef communities that were mapped from the satellite image classification but for which there are no published values relating specifically to Lizard Island. In such cases, published values for other sites were employed, including calcified macroalgae (e.g. *Halimeda*) (Harney and Fletcher, 2003) and seagrass (Perry and Beavington-Penny, 2005). Where mapped classes comprised a composite of benthic assemblages, census-based estimates of community calcification were derived by summing across the different benthic components present, see Equation 2 (observed benthic coverages are listed in Table 2). To convert carbonate production rates for each benthic cover to reef accretion, individual values were divided by their density. Published density values were input

for live coral, algae, rubble, sand, calcified algae and encrusting coral (Kinsey, 1979; Hubbard, 1985; Montaggioni and Braithwaite, 2009). It was estimated that 25% of community calcification at Lizard Island is converted into upward reef platform accretion, with the remaining portion being either bioeroded or mechanically broken down and transported to other settings within the reef system. This value was based on framework construction estimates from other reefs (Hubbard, 1985). The relative proportion of each biotic component was ascertained from the field dataset of 364 video footage records. Records were subdivided on the basis of the mapped benthic cover class in which they fell and the average coverage was calculated for each benthic cover class. For each benthic class, potential production values were converted into corresponding reef platform accretion and overall reef accretion, G_a, was calculated by summing across the relative proportion (Table 2) of the n biotic components that made up the assemblages (P_i) (Equation 2):

$$G_a = 0.01 \times \sum_{i=1}^{n} (P_i \times \%\ \text{cover}) \qquad \text{Equation 2}$$

Simulation model construction and implementation

The digital terrain model that represented the modern topographic configuration of the reef platform around Lizard Island formed the basis over which successive decades of accretion were added. The modern benthic biological community occupying the reef surface, was captured in the benthic cover map. The simulation model was a cellular automata model implemented for nine time steps spanning 2011 – 2100. For each cell, the upward reef accretion, G_a was calculated for the given time step depending on the benthic cover and added to the existing digital terrain model of the reef platform. Sea-level rise across an equivalent time step was subtracted at a linear rate over the 21st Century to generate a new digital terrain model indicating the vertical position of the reef platform relative to the surface at time step 2 (Equation 3).

$$Z_2 = Z_1 + G_a - \mathrm{SLR}_1 \qquad \text{Equation 3}$$

Where Z_2 = cell water depth at time step 2 (m)

Z_1 = cell water depth at time step 1 (m)

G_a= cell upward reef accretion during time interval 1 to 2 (equation 2).

SLR_1= sea level rise during time interval 1 to 2.

Three rules were applied by inserting Boolean conditional statements into the model to reconfigure the benthic cover type in between each simulation time step, which were based on geomorphic transitions associated with particular depth ranges across reefs (Hopley, 1993, 1997) and parameterised on the basis of the existing depth ranges of the geomorphic zones evident at Lizard Island. The first rule (Rule #1) stated that any area of the reef platform above a depth of - 1.7 m, which coincided with the limiting mean low water springs height, did not accrete upwards as it was vertically constrained by tidal exposure. The second rule (Rule #2) stated that if a new depth that fell in the range - 1.7 – - 6.0m was achieved for a cell that had previously been attributed to a tidally limited reef flat class, the cover type changed to a coral dominated reef. This captured the transition in suitability of the reef flat for coral survival as inundation progressed with the differing sea-level rise scenarios. Finally, a third rule (Rule #3) captured any deeper benthic reef components and stated that for any area of the reef where the depth exceeded 18m, there would be no further accretion. On the basis of the existing depth limit of accretionary benthic substrates as identified from the benthic map, this captured the point at which reef surfaces lagged behind the rate of sea-level rise and began to slowly drown.

Results

The WorldView-2 satellite image was largely free of cloud and glint, and it clearly depicted many of the subsurface features of the reef platform. Figure 3 shows the benthic surface cover map of the complete reef platform (area 16.7 km^2) around Lizard Island, the overall

accuracy (Congalton, 1991) of which was found to be 82 % on the basis of the remaining 314 video footage samples that were not used for supervising (calibrating) the image classification, but kept back as an independent validation dataset.

Live coral is largely restricted to the outer reef slope and crest, forming a near continuous band around the entire barrier and fringing reef system. The reef is most developed on the windward side, particularly across the southeast-facing reef front and adjacent to Coconut Beach, while the reefs on the western side, such as those in Watson's Bay, tend to be restricted to patches. Reef flats tend to be dominated by coral, soft coral and calcified algae, whereas the deeper lagoon areas are composed predominantly of sand with varying proportions of algae and rubble. The shallower lagoon areas comprise a matrix of sand with coral patches, sparse coral, rubble seagrass and algae.

Many of the benthic classes mapped were dominated by sand (>80% cover) with varying proportions of algae, seagrass, coral and rubble (classes 4 and 7 – 10) and consequently were associated with a low rate of carbonate production. These classes were primarily distributed inside the lagoon and across the deeper forereef slope areas. Other classes (5, 6) were dominated by turf algae, dead coral framework or seagrass beds, which also had a low rate of carbonate production. The classes with the highest rates of carbonate production (1–3) encompassed a high proportion (>30%) of live coral, encrusting calcified algae and calcified macroalgae and were primarily distributed across the shallower reef flat and forereef areas.

Simulation model construction and implementation

Figure 4 shows the simulated response to a sea-level rise of 0.5 m by the year 2100. There is a gradual shallowing of the reef platform surface as the reef flat becomes colonised with corals that accrete faster than the existing coral, soft coral and calcified algal composite of benthic

surface cover. This is due in large part to the increased water depth over the reef flat, resulting in much of this area becoming inundated throughout the tidal cycle, thus, the vertical constraints that previously limited coral growth are gradually removed across the ninety year period simulated. A similar situation can be seen on the surface of the reef patches along the western side of the island and across the shallow extensive reef flat on the west side of the lagoon, which was previously occupied by sparse coral, rubble and algal substrate. Other benthic classes appear to have a mixed response to this rate of rise with some of the deeper zones, such as the shelf platform to the west of the island and the lagoon floor failing to keep up with the rise.

Figures 5 shows the simulated response to a more rapid rate of sea-level rise of 1.2m by 2100. As with the 0.5m rise, the overall reef system appears to progress more rapidly through an initial stage of reef flat coral colonisation, resulting in the shallow platform surfaces for the first 30-40 years. However, the effects of this initial reef flat inundation are lessened as the relative position of the sea surface rises in relation to the platform surface and the reef platform slowly begins to lag behind, a trajectory on which it continues until the end of the simulation period in 2100.

Figure 6 illustrates the characteristic behaviour of transects traversing each of the study sites across the simulation period. The southeast reef flat simulation yields some interesting patterns in relation to these broader scale transitions (Fig. 6a). In the case of the 0.5m rise scenario, both the reef flat and slope are able to keep up with the sea surface and accrete above the level of their modern profile in accordance with the calcification rate of the benthic cover occupying these zones. Deeper lagoon and forereef zones display a rate of rise that is commensurate with the sea surface. Thus, it would appear that, over time, those platform areas occupied by the benthic surfaces with greater accretion rates (i.e. coral) will become

raised at a rate greater than their surrounding platform surfaces, accentuating the existing topography. A similar phenomenon is observable along the reef crest at Coconut Beach (Fig. 6b) and across the mid-bay reef platform that dissects the Watson's Bay transect (Fig. 6c). For the 1.2 m rise scenario, in all cases the 2100 reef platform profile is above its modern level, however, it is deeper with respect to the rising sea level. The extent to which it has deepened is dependent on the benthic cover of the platform surface with benthic covers that accrete at a low rate (e.g. the sandy platforms of Mangrove Beach and Watson's Bay) lagging further behind than coral patches. Uniform change of this nature can be seen across the largely homogenous transects at Mangrove Beach and Watson's Bay.

Discussion

For the overall Lizard Island reef system, simulations indicate that the shallow, coral dominated reef platform coincides with the more active areas of carbonate production and is able to keep up with a sea-level rise rate of 0.5 m by 2100 for the complete simulation period (2011 – 2100) whereas the other platform areas dominated by sand get progressively deeper. This response of the active shallow areas, largely controlled by the geomorphic transitional rule stating that shallow reef flats will be recolonised by coral, is contingent on the ability of corals to occupy these newly inundated shallow platforms, which may be compromised on other reefs due to additional anthropogenic stressors such as pollution (Burke et al, 2011). For the rate of 1.2 m rise by 2100, the whole platform initially keeps up with the rise, then begins to drown. Deeper areas such as the central lagoon floor and the shelf to the west of the island are occupied by substrates such as sand, algae and low density seagrass that accrete at a relatively low rate (≈1 mm yr^{-1}), the platform becomes deeper relative to sea level, whereas in the initial stages of the simulation period, it tracks sea level and displays catch-up behaviour for shallower areas.

A comparison of the simulated response across the different reef platform settings provides insight into how reef platforms may respond, both in other areas of the GBR and across the wider reef seas. The presence of a reef platform (i.e. the fringing reef at Coconut Beach or the Southeast reef flat) provides a shallow benthic surface suitable for coral larval settlement and growth at a point when the platform becomes permanently inundated throughout the tidal cycle. This colonisation by organisms that produce carbonate at a comparatively fast rate (coral, calcified algae) enables the whole shallow reef platform to remain close to sea level. Where there is no reef platform present (i.e. at Watson's Bay and Mangrove Beach), much of the benthic surface is less productive and cannot keep pace with sea-level rise, as is evidenced by the lack of carbonate sands on the beaches at these quartz dominated sites, with a carbonate content of 0-20% at Mangrove Beach and 40-50% at Watson's Bay as opposed to 70-90% at Coconut Beach (Webster, 1993).

The different types of reef platform setting exemplified by the southeast reef flat, Coconut Beach and Watson's Bay illustrate a gradient of reef platform response related to accretion rate, whereby coral-dominated features with high accretion rates become more prominent, those with moderate accretion rates (reef flat and forereef) accrete upwards at a rate commensurate with the rate of rise, thereby maintaining their original profile and position relative to the sea surface and those with a low accretion rate (lagoon floor and western shelf) maintain a similar profile but slowly gain depth relative to sea-level. The result of this variable response is that elevated features of the reef platform, such as reef patches and crests tend to become more pronounced, as can be seen in the simulation profiles for the Southeast reef flat, Coconut Beach and Watson's Bay. This phenomenon has commonly been interpreted as underpinning past reef behaviour in response to sea-level rise (Davies, 2011).

The overall trajectories observed have several implications for reefs, both across the Great Barrier Reef province and the wider Indo-Pacific region. Although there does not appear to be

evidence of higher sea level preserved on Lizard Island, the coincidence of the modern reef profile with mean low water springs (MLWS) indicates that the reef flats are close to or limited in their upward growth by exposure to the atmosphere during the low water stages of the tidal cycle. This is the case for many emergent Indo-Pacific reef platforms which are exposed during low tides, including annular Pacific atoll reefs such as Rennell (Solomon Islands), Mare (Vanuatu) and Niue (Dickinson, 2004), the northern Great Barrier Reef (Larcombe et al., 1995), northern Queensland (Chappell, 1983) the Torres Strait reefs, including Yam, Warraber and Hammond Island (Woodroffe et al., 2000), Magnetic Island (Yu and Zhao, 2009) and Bewick Island (Kench et al., 2012). Such platforms are characterised by broad windward reef flats that are emergent at low tide, an emergence that has been exacerbated either by tectonic uplift or a slight fall of relative sea level, leaving mid-Holocene (6-3 ka) shorelines 1-2 m above the present sea level (Hopley et al., 2007). For such elevated reefs, the existence of a negative feedback effect will likely delay drowning of shallow geomorphological zones. The time lag afforded by this negative feedback before the reef platform begins to drown is notable, the minimum length of which appears to be around 40 years for the most extreme sea-level rise scenario (1.2 m by 2100) but which likely extends beyond 2100 for lesser rates of rise and for reef flats that are elevated above modern sea level.

While it is difficult to validate the simulations, it is instructive to examine evidence of past historical accretionary dynamics, such as available core data, surface deposits and radiocarbon dated sediment samples taken from different settings within the reef platform to ascertain the correspondence of future simulated behaviour with past behaviour. For example, in the case of the Southeast reef flat setting, suspended sediment studies suggest negligible horizontal build out of the windward forereef, with removal rates more than accounting for any net carbonate production on the windward reef (Davies, 1977). Drilling results from three cores sunk into the southeasternmost reef flat on Lizard Island, just east of South Island lend

support for insignificant horizontal windward reef accretion. Recovery was poor, but the deepest borehole reached 4.5 m at which depth it was considered that the underlying granite had been encountered (Rees et al., 2006). A date on coral at the base of that core of 6722±243 years BP is consistent with reef initiation at this depth, whereas a date of 4830±331 years BP on a shallower core appears younger than expected. Both cores, however, were topped by modern coral indicating a history of ongoing vertical reef accretion at growth rates averaging at least 0.5-0.7 mm/yr. This growth signature is inferred to have lagged a little, experiencing a catch-up mode of development (Rees et al., 2006) and such a pattern appears to continue across the period simulated, indicating continuity of historical reef platform accretion dynamics.

This study has focussed on the accretion of reef framework in response to sea-level rise; it is important to note that the simulations presented do not account for any portion of the carbonate budget that is either *i.* lost from its site of production, or *ii.* imported from elsewhere in the reef system. In this sense, the model simulates the accretion of consolidated reef framework as opposed to unconsolidated sedimentary landforms. At other sites it has been assumed that about half the production is shed (Hubbard, 1985, Hart and Kench, 2007). In the context of Lizard Island, measurements of suspended sediment transport across the reef on ebb and flood tides have led to the suggestion that all the carbonate produced (suspended and unconsolidated coarse sediment and rubble) on the windward reef is removed leeward by the rapid water movement across this reef to contribute to progradation on the western margin of the reef north of Palfrey Island (LIMER, 1975; Davies, 1977). It seems likely that a large proportion of this carbonate is deposited in the lagoon before reaching the western reef margin. Additional loss of material from productive windward reefs is evident from records of large reef detritus exported down the western reef front and collected in trays over the period 1991-1995 from which it was estimated that the reef margin loses approximately 2 kg of

carbonate material down the reef front per metre per year (Hughes, 1999). In addition to the mechanical movement of carbonate sand toward inshore depositional areas such as Coconut Beach, bioerosion is an important component contributing to loss from the material budget. Studies have yielded variable estimates of the rate of bioerosion at Lizard Island, including up to 2.7 kg m^{-2} yr^{-1} through experiments that deployed coral blocks at various subtidal sites (Kiene and Hutchings, 1992, 1994), with the amount of bioerosion by parrotfish alone estimated for different sites as up to 5.6 kg m^{-2} yr^{-1} at the southeast side of the South Island (Bellwood, 1995a) and up to 10 kg m^{-2} yr^{-1} at the northern end of the island (Bellwood, 1995b, 1996). In addition, boring by polychaetes and sipuncular worms, sponges and molluscs will also contribute to bioerosion rates, with microborers including endolith algal communities and euendolithic fungi eroding the reef at a rate of 0.71 kg m^{-2} yr^{-1} (Trillobet and Golubic, 2005). Thus, a more complete representation of the carbonate budget might seek to quantify the movements of sediment both within the reef system and that exported from the system altogether.

Potential decrease in the rate of carbonate production due to ocean acidification could result in significant variation in the simulated position of the reef platform relative to sea level (Kleypas and Langdon, 2006). Evidence from the skeletal records of 328 *Porites* colonies on the GBR suggests that their rate of calcification has declined by 14.2% since 1990 with the likely cause being the declining saturation state of seawater aragonite which may be reducing the ability of GBR corals to calcify (De'ath et al., 2009). Given that most of the hydrochemically-derived estimates of reef calcification at Lizard Island are over ten years old (LIMER, 1975; Smith and Kinsey, 1976; Chisholm, 2000), there is a pressing need to update these measurements that underpin the platform simulations.

Conclusions

The key findings of the simulations conducted in the present paper are as follows:

1. For a sea-level rise scenario of 0.5 m by 2100, shallow reef platform areas colonised by organisms that produce carbonate at a relatively fast rate appear to be able to keep pace with a rising sea, whereas for a rise of 1.2 m by 2100 these areas keep pace for approximately 40 years and then begin to drown.
2. Reef platform features with high accretion rates (i.e. coral patches and reef crests) have a tendency to become more pronounced in the landscape due to their ability to keep pace with a rising sea, while other features (e.g. the sandy lagoon floor) drown.
3. Reef flats that are close to modern sea level, of which there are many examples across the Indo-Pacific region, may become recolonized by corals as they become inundated throughout the tidal cycle, enhancing their ability to accrete upward. This negative feedback will result in shallow reef platforms being able to keep pace with a rising sea level.

The model simulations are based on the observation that morphological change in reef configuration over time is dependent on four properties: *i.* the time of initiation of reef growth, *ii.* the shape and depth of the surface from which the reef grew, *iii.* the rate of reef growth, and *iv.* the relationship between reef growth and sea level change (Kinsey and Davies, 1975). The first two of these properties are captured in the high resolution digital terrain model while the benthic surface cover map captures the third by providing a spatially continuous, high resolution record of the benthic community that can be related to corresponding rates of platform accretion. This updates existing benthic community records for Lizard Island (Pichon and Morrissey, 1981; Nelson, 1992) and uses these to estimate total carbonate production for the complete reef system through the combination of remote sensing with census-based approaches (Andrefouet and Payri, 2000; Vescei, 2001, 2004; Moses et al., 2009; Leon and Woodroffe, 2012). The simulation models go beyond estimating carbonate production by bringing these key components of reef platform evolution together with projections of how sea

levels will rise over the course of the next century, thus, completing the picture in terms of gross morphological change of reefs as three-dimensional structures. To parameterise simulations with high resolution digital terrain models and benthic surface cover maps enables the response of reef platforms to be modelled in a more deterministic or realistic manner than has been used in previous simulations of reef community dynamics (Blanchon and Blakeway, 2003; Langmead and Sheppard, 2004). Such an approach draws on available information to establish key boundary conditions for a platform configuration that is comparable to regional reef systems and could be further used to predict related patterns of island deposition or erosion in inverse or optimisation models that encompass the mobile portion of the carbonate budget, for example, sediment allocation models (Barry et al., 2007, 2008). In this sense, the present study provides a useful starting point for future modelling exercises of the response of reef platforms to sea-level rise as data on rates of rise, carbonate production and elevation models of other reef platforms become available.

Acknowledgements

This work has been made possible by a Lizard Island Research Station Fellowship grant, 2011 and a University of Wollongong URC grant, 2011 to SH. Professor Valerie Harwood is thanked for assistance with fieldwork. MIS and JL were supported by an Australian Research Council SuperScience Grant awarded to the Global Change Institute and University of Queensland New Staff Research Start-Up Funds. The research was motivated by involvement with members of the Australian Sea Level Rise Partnership.

References

Andrefouet, S., Payri, C., 2000. Scaling-up carbon and carbonate metabolism of coral reefs using in-situ data and remote sensing. Coral reefs 19, 259-269.

Barry, S, Cowell, P., Woodroffe, C., 2007. A morphodynamic model of reef island development on atolls. Sedimentary Geology 197, 47-63

Barry, S, Cowell, P., Woodroffe, C., 2008. Growth-limiting size of atoll-islets: Morphodynamics in nature. Marine Geology 247, 159-177

Bellwood, D.R., 1995a. Direct estimate of bioerosion by two parrotfish species, *Chlorurus gibbus* and *C. sordidus*, on the Great Barrier Reef. Australian Marine Biology 121, 419-429.

Bellwood, D.R., 1995b. Carbonate transport and within-reef patterns of bioerosion and sediment release by parrotfishes (family Scaridae) on the Great Barrier Reef. Marine Ecology Progress Series 117, 127-136.

Bellwood, D.R., 1996. Production and reworking of sediment by parrotfishes (family Scaridae) on the Great Barrier Reef. Marine Biology 125, 795-800.

Blanchon, P., Blakeway, D., 2003. Are catch-up reefs an artifact of coring? Sedimentology 50, 1271–1282

Blanchon, P., Eisenhauer, A., Fietzke, J., Liebetrau, V., 2009. Rapid sea-level rise and reef back-stepping at the close of the last interglacial highstand. Nature Letters 458, 881-885.
Buddemeier R., Smith S., 1988. Coral reef growth in an era of rapidly rising sea level: predictions and suggestions for long-term research. Coral Reefs 7, 51-56
Burke, L., Reytar, K., Spalding, M., Perry, A., 2011. Reefs at Risk revisited. Publication of the World Resources Institute, Washingotn, 130pp.
Chappell, J., 1983. Evidence for smoothly falling sea level relative to North Queensland, Australia, during the past 6000 yr. Nature 302, 406–408.
Chave, K.E., Smith, S.V., Roy, K.J., 1972. Carbonate production by coral reefs. Marine Geology 12, 123-140.
Chisholm, J.R., 2000. Calcification by crustose coralline algae on the northern Great Barrier Reef, Australia. Limnol. Oceanogr 45, 1476-1484.
Church J.A., White N.J., 2006. A 20th century acceleration in global sea level rise, Geophysical Research Letters. 33, L01602, 4 PP., 2006 doi:10.1029/2005GL024826
Congalton, R., 1991. A Review of Assessing the Accuracy of Classifications of Remotely Sensed Data. Remote Sensing of the Environment 29, 35-46.
Cooley, T., Anderson, G.P., Felde, G.W., Hoke, M.L, Ratowski, A.J., Chetwynd, JH, Gardner, J.A., Adler-Golden, SM, Matthew, M.W., Bernstein, L.S, Achara, P.K, Miller, D., Lewis, P., 2002. FLAASH: A MODTRAN4-based Atmospheric Correction Algorithm, Its Application and Validation. Proceedings of the IEEE Symposium on Geoscience and Remote Sensing, pp 145-158.
Coleman, J.B., Yao, X.B., Jordan, T.R., Madden, M., 2011. Holes in the ocean: Filling voids in bathymetric lidar data. Computers & Geosciences 37, 474-484.
Daly, M., 2005. Wave energy and shoreline response on a fringing reef complex, Lizard Island, Qld, Australia. Unpublished B Env Sci thesis, University of New South Wales, Sydney, 105 pp.
Davies, P.J., 1977. Modern reef growth – Great Barrier Reef. Proceedings of the Third International Coral Reef Symposium, v. 2, pp. 325-330.
Davies, P.J., Montaggioni, L.F., 1985. Reef growth and sea-level change: the environmental signature. Proceedings of the 5th International Coral Reef Congress. Tahiti, French Polynesia, 3, 477-515.
Davies, P.J., 2011. Antecedent Platforms. In: Hopley, D (Ed.) Encyclopedia of Modern Coral Reefs: Structure, Form and Process, Springer-Verlag, Berlin. pp 40-46.
De'ath, G, Lough, J., Fabricius, K.E., 2009. Declining coral calcification on the Great Barrier Reef. Science 323, 116-119.
Dickinson, W.R., 2004. Impacts of eustasy and hydro-isostasy on the evolution and landforms of Pacific atolls. Palaeogeography, Palaeoclimatology, Palaeoecology 213, 251-269.
Done, T.J., 2011. Corals: Environmental Controls on growth. In: Hopley, D (Ed.) Encyclopedia of Modern Coral Reefs: Structure, Form and Process, Springer-Verlag, Berlin. pp 281-293.
Dullo W.C., 2005. Coral growth and reef growth: a brief review. Facies 51, 33-48
Harney, J.N., Fletcher C.H., 2003, A budget of carbonate framework and sediment production, Kailua Bay, Oahu, Hawaii. Journal of Sedimentary Research. 73, 856-868.
Hart, D.E., Kench, P.S., 2007. Carbonate production of an emergent reef platform, Warraber Island, Torres Strait, Australia. Coral Reefs 26, 53-68.
Hengl, T., Bajat, B., Blagojevic, D., Reuter, H.I., 2008. Geostatistical modeling of topography using auxiliary maps. Computers & Geosciences 34, 1886-1899.
Hopley, D., 1993. Coral reefs in a period of global sea level rise. In: Saxena N.K. (Ed.), Recent advances in marine science and technology. PACON, Honolulu, pp. 453-462.
Hopley, D., 1997. Coral reef islands: implications of more modest global change predictions. In: Sexena, N. (Ed) Recent advances in marine science and technology, Proc. Pacific Congress on Marine Science and Technology, Honolulu, pp. 249-258.

Hopley, D., Smithers, S.G., Parnell, K.E., 2007. The geomorphology of the Great Barrier Reef: Development, Diversity and Change. Cambridge University Press, Cambridge, 532 pp.
Hubbard, D.K., 1985. What do we mean by reef growth? Proceedings of the Fifth International Coral Reef Congress, Tahiti. 6,433- 438.
Hubbard, D.K., 1997. Reefs as dynamic systems. In: Birkeland, C. (Ed.), Life and Death of Coral Reefs. Chapman & Hall, New York, pp. 43-67.
Hughes, T.P., 1999. Off-reef transport of coral fragments at Lizard Island, Australia. Marine Geology 157, 1-6.
Hughes, T.P., Baird, A.H., Bellwood, D.R., Card, M., Connolly, S.R., Folke, C., Grosberg, R., Hoegh-Guldberg, O., Jackson, J.B.C., Kleypas, J., Lough, J.M., Marshall, P., Nystrom, M., Palumbi, S.R., Pandoli, J.M., Rosen, B., Roughgarden, J., 2003. Climate change, human impacts, and the resilience of coral reefs. Science 301, 929-933.
Intergovernmental Panel on Climate Change (IPCC)., 2007. Synthesis Report. Contribution of Working Groups I, II and III to the Fourth Assessment Report of the Intergovernmental Panel on Climate Change. Geneva, Switzerland.
Kinsey, D.W., 1979. Carbon turnover and accumulation by coral reefs, PhD Thesis, University of Hawaii, 248 pp.
Kench, P.S., Smithers, S.G., McLean, R.F., 2012. Rapid reef island formation and stability over an emerging reef flat: Bewick Cay, northern Great Barrier Reef, Australia. Geology 40, 347-350.
Kiene, W.S., Hutchings, P.A., 1992. Long-term bioerosion of experimental coral substrates from Lizard Island, Great Barrier Reef. Proceedings of the Seventh International Coral Reef Symposium, v. 1, Guam, Micronesia, p. 397-403.
Kiene, W.S., Hutchings, P.A., 1994. Bioerosion experiments at Lizard Island, Great Barrier Reef. Coral Reefs 13, 91-98.
Kinsey, D.W. Davies, P.J., 1975. Coral Reef Growth- A model based on morphological and metabolic studies, Australian Journal of Marine Science, 7, 397-403.
Kinsey, D.W., 1985. Metabolism, calcification and carbon production I System Level Studies, Proceedings of the 5th Coral Reef Congress, Tahiti, French Polynesia, 4, 505 – 526.
Kleypas, J., Langdon, C., 2006. Coral reefs and changing seawater chemistry. In Phinney, J. T. (Ed.) Coral Reefs and Climate Change, Washington, DC: American Geophysical Union, pp. 73–110.
Langmead, O., Sheppard, C., 2004. Coral Reef community dynamics and disturbance: A simulation model. Ecological Modelling 3, 271-290.
Larcombe, P., Carter, R.M., Dye, J., Gagan, M.K., Johnson, D.P., 1995. New evidence for episodic postglacial sea-level rise, Central Great-Barrier-Reef, Australia. Marine Geology 127, 1–44.
Leon, J, Woodroffe, C., 2012. Morphological characterisation of reef types in Torres Strait and an assessment of their carbonate production. Marine Geology DOI: 10.1016/j.margeo.2012.12.009
Leon, J., Phinn, S.R, Hamylton, S., Saunders, M., 2013. Filling the 'white ribbon': A seamless multisource digital elevation / depth model for Lizard Island, northern Great Barrier Reef. International Journal of Remote Sensing 34, 6337-6354.
LIMER Expedition Team, 1975. Metabolic processes of coral reef communities at Lizard Island, Queensland. Search 7, 463-468.
Madin, J.S., Black, K.P., Connolly, S.R., 2006. Scaling water motion on coral reefs: from regional to organismal scales. Coral Reefs 25, 635-644.
Mitrovica, J.X., Milne, G.A., 2002. On the origin of late Holocene sea-level highstands within equatorial ocean basins. Quaternary Science Reviews 21, 2179-2190.
Montaggioni, LF, Braithwaite, CJR, 2009. Quaternary Coral Reef Systems: History, Development processes and controlling factors, Developments in Marine Geology, Elsevier, Oxford, 362 pp.

Moses, C.S., Andrefouet, S., Kranenburg, C.J., Muller-Karger, F.E., 2009. Regional Estimates of reef carbonate dynamics and productivity using Landsat 7 ETM+ and potential impacts from ocean acidification. Marine Ecology Progress Series 380, 105-115.
Nelson, V.V., 1992. Patterns of Cover, Diversity and Spatial Arrangement of Benthos at Lizard Island, Great Barrier Reef, Proceedings of the Seventh International Coral Reef Symposium, Guam, Micronesia, 1992, Vol. 2,pp.3965-4121.
Neumann, A.C., Macintyre, I., 1985. Reef response to sea level rise: keep-up, catch-up or give-up. Proceedings of the 5th International Coral Reef Congress. 3, 105-110.
Nicholls, R.J., Marinova, N., Lowe, J.A., Brown, S., Vellinga, P., Gusmao, D., Hinkel, J., Tol, R.S.J., 2011.Sea-level rise and its possible impacts given a 'beyond 4°C world' in the twenty-first century. Philosophical Transactions of the Royal Society A. 1934, 161-181.
Perry, C., Beavington-Penney, S.J. 2005. Epiphytic calcium carbonate production and facies development within sub-tropical seagrass beds, Inhaca Island, Mozambique. Sedimentary Geology 174, 161-176.
Pichon, M., Morrisey, J., 1981. Benthic Zonation and Community Structure of South Island Reef, Lizard Island (Great Barrier Reef). Bulletin of Marine Science 31, 581-593.
Rahmstorf S., 2007a. Degrees of change. Nature 448, 136-136.
Rahmstorf S., 2007b. A Semi-Empirical Approach to Projecting Future Sea-Level Rise. Science 315, 368-370.
Rees, S.A., Opdyke, B.N., Wilson, P.A., Fifield, L.K., Levchenko, V., 2006. Holocene evolution of the granite based Lizard Island and MacGillivray systems, northern Great Barrier Reef. Coral Reefs 25, 555-565.
Smith, S.V., Kinsey, D.W., 1976. Calcium carbonate production, coral reef growth, and sea level change. Science 194, 937-939.
Smith, S.V., Wiebe, W.J., 1977. Rates of Carbon fixation, organic Carbon release and Translocation in a Reef-building Foraminifer, *Marginopora vertebralis.* Australian Journal of Marine and Freshwater Research 28, 311-319.
Sheppard, C.S., Dixon, D.J., Gourlay, M., Sheppard, A., Payet, R., 2005. Coral mortality increases wave energy reaching shores protected by reef flats: Examples from the Seychelles. Estuarine, Coastal and Shelf Science 64, 223-234.
Scopélitis, J., Andréfouët, S., Phinn, S., Done, T., Chabanet, P., 2011. Coral colonisation of a shallow reef flat in response to rising sea level: quantification from 35 years of remote sensing data at Heron Island, Australia. Coral Reefs 30: 951-965.
Trillobet, A., Golubic, S., 2005. Cross-shelf differences in the pattern and pace of bioerosion of experimental carbonate substrates exposed for 3 years on the northern Great Barrier Reef, Australia. Coral Reefs 24, 422-434.
Silverman, J., Lazar, B. Erez, J., 2007. Effect of aragonite saturation, temperature, and nutrients on the community calcification rate of a coral reef. Journal of Geophysical Research 112, C05004, doi:10.1029/2006JC003770.
Stoddart D, McLean, R.F., Scoffin, T.P., Thom B.G., Hopley, D., 1978. Evolution of Reefs and Islands, Northern Great Barrier Reef: Synthesis and Interpretation. Phil. Trans. Roy. Soc. London B 284, 149-159.
Smithers, S.G., Woodroffe, C.D., 2001. Coral microatolls and 20th century sea level in the eastern Indian Ocean. Earth and Planetary Science Letters 191, 173-184.
Vescei, A., 2001. Forereef carbonate production: Development of a regional census-based method and first estimates, Palaeogeography, Palaeoclimatology 175, 185-200
Vescei, A., 2004. A new estimate of global reefal carbonate production including forereefs. Global and Planetary change 43, 1-18.
Webster, J., 1993. Siliciclastic/carbonate interactions at Lizard Island, in the northern Great Barrier Reef. Unpublished BSc Honours thesis, University of Sydney. 185pp.
Woodroffe, C.D., Kennedy, D.M., Hopley, D., Rasmussen, C.E., Smithers S.G., 2000. Holocene reef growth in Torres Strait. Marine Geology 170, 331-346.

Woodroffe, C.D., 2007. Critical thresholds and the vulnerability of Australian tropical coastal ecosystems to the impacts of climate change. Journal of Coastal Research 50, 469-473.
Woodroffe, C.D., 2008. Reef-island topography and the vulnerability of atolls to sea-level rise. Global and Planetary Change 62, 77-96.
Yu, K., Zhao, J., 2009. U-series dates of Great Barrier Reef corals suggest at least +0.7 m sea level ~7000 years ago. The Holocene 20, 161-168.

List of figures

Figure 1. A WorldView-2 satellite image of Lizard Island (145°27'145" E; 14°40'12" S). The dots depict video ground referencing points and the red lines depict four reef profile transects adopted for the present assessment of sea-level rise. Inset: Location of Lizard Island along the Queensland coastline.

Figure 2 A digital terrain model of Lizard Island and the surrounding reef system (vertical exaggeration factor 5).

Figure 3. The benthic cover map of the reef platform at Lizard Island derived from the classification of the WorldView-2 satellite image.

Figure 4 Simulated reef platform bathymetry under a sea-level rise scenario of 0.5 m above 1990 levels by 2100. The reef flat (which was previously exposed throughout the tidal cycle) becomes permanently inundated and is colonised by corals, which accrete rapidly and enable shallow surfaces to remain shallow.

Figure 5 Simulated reef platform bathymetry under a sea-level rise scenario of 1.2 m above 1990 levels by 2100. As with the 0.5 m scenario, the reef flat is colonised by corals within a shorter timeframe, however, they cannot keep up with the pace of sea-level rise and the reef platform begins to drown at approximately 2050.

Figure 6 Reef profile transects depicting the modern reef profile and the 2100 profile with a 0.5 m sea-level rise and a 1.2 sea-level rise for a) the South-East reef flat, b) Coconut Beach, c) Watson's Bay, and d) Mangrove Beach. Note: Values are plotted in relation to current sea level, however, the 2100 sea level is marked on each plot to illustrate differing depths above the reef platform surface. The y-axis labels may vary between the 0.5 and 1.2 m scenarios.

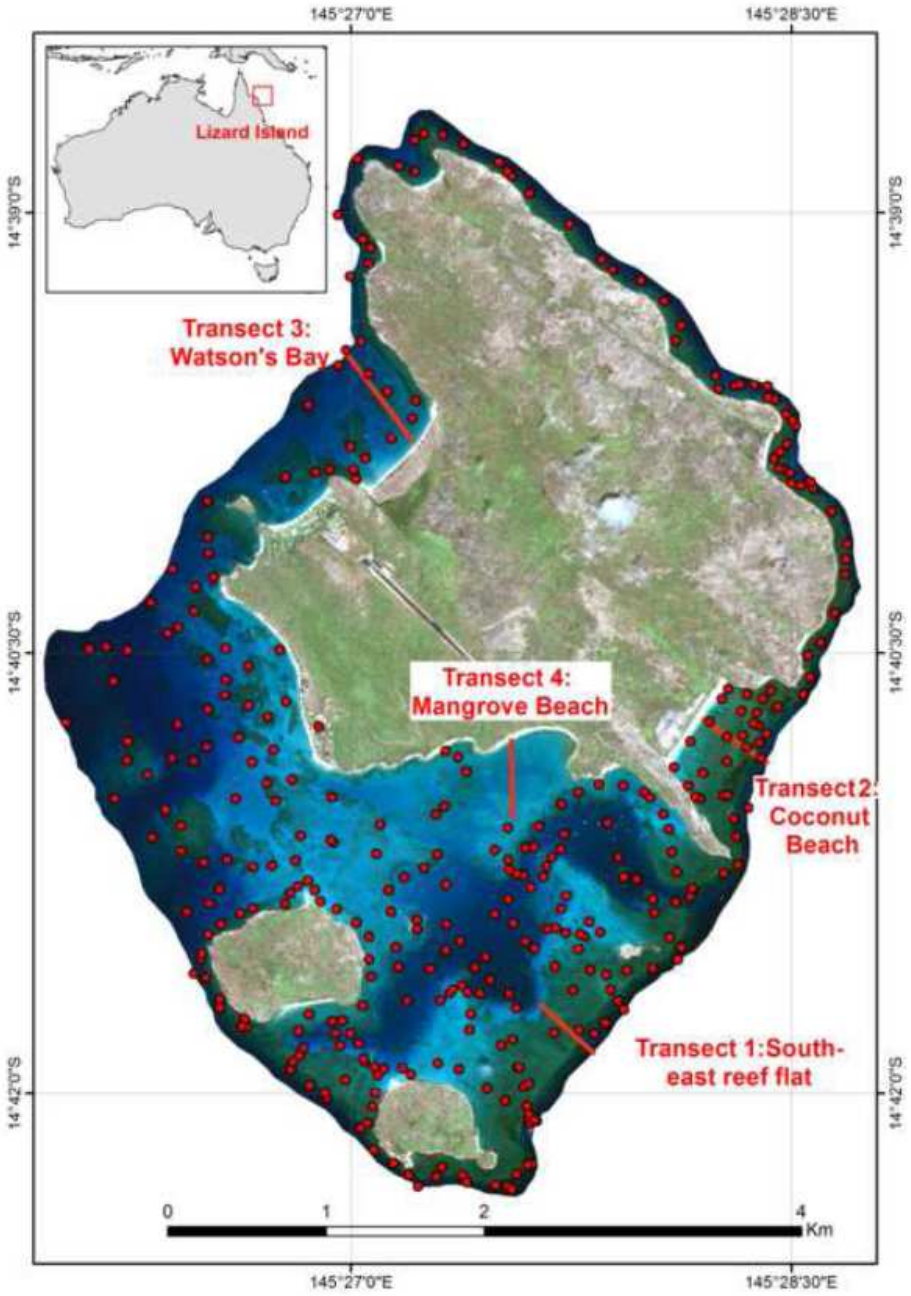

Figure 1

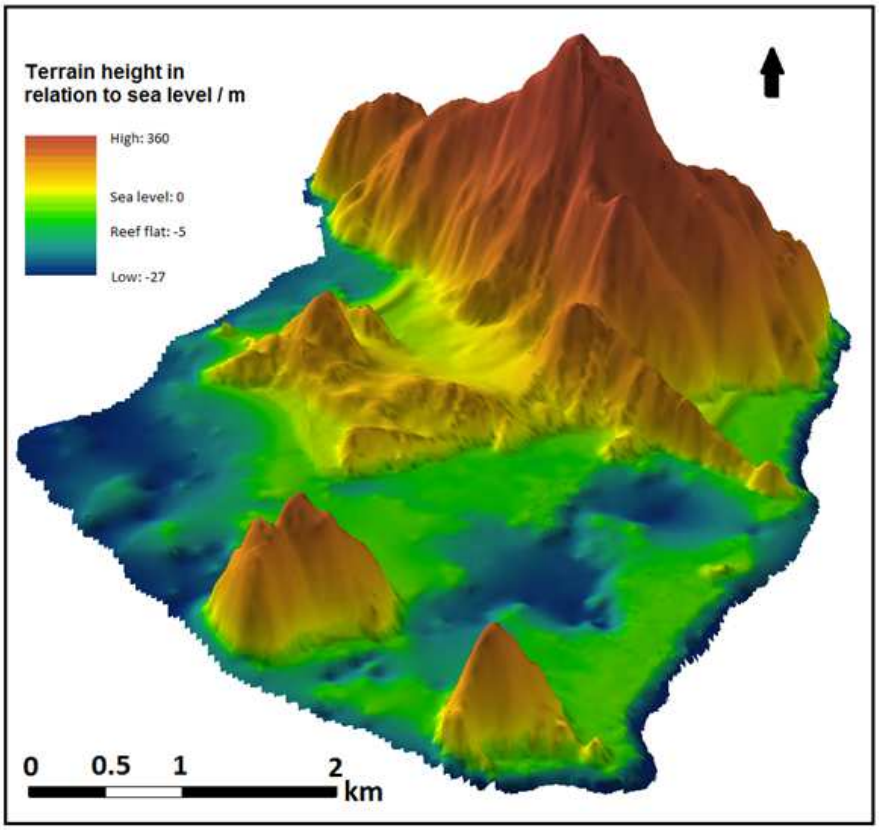

Figure 2

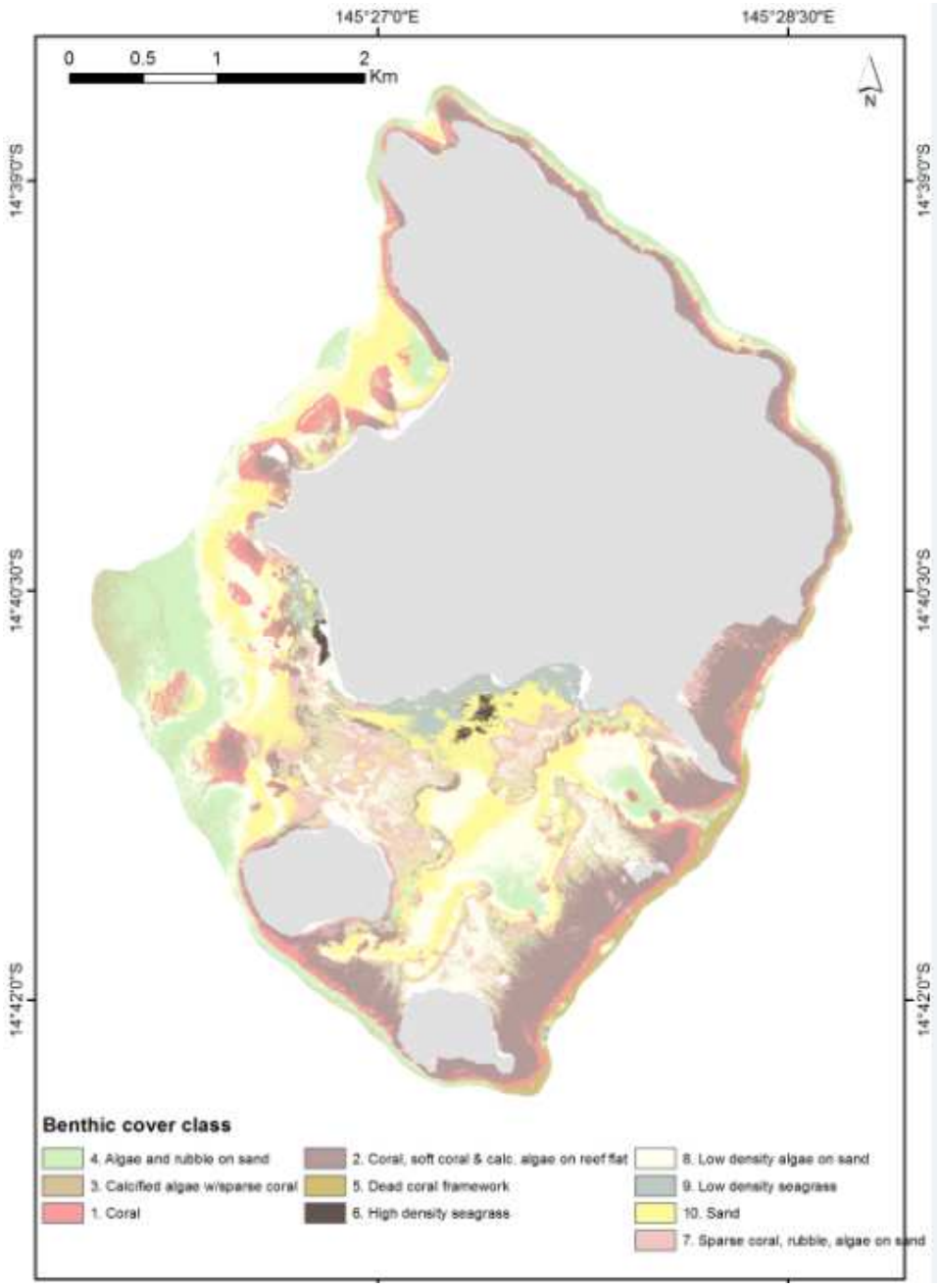

Figure 3

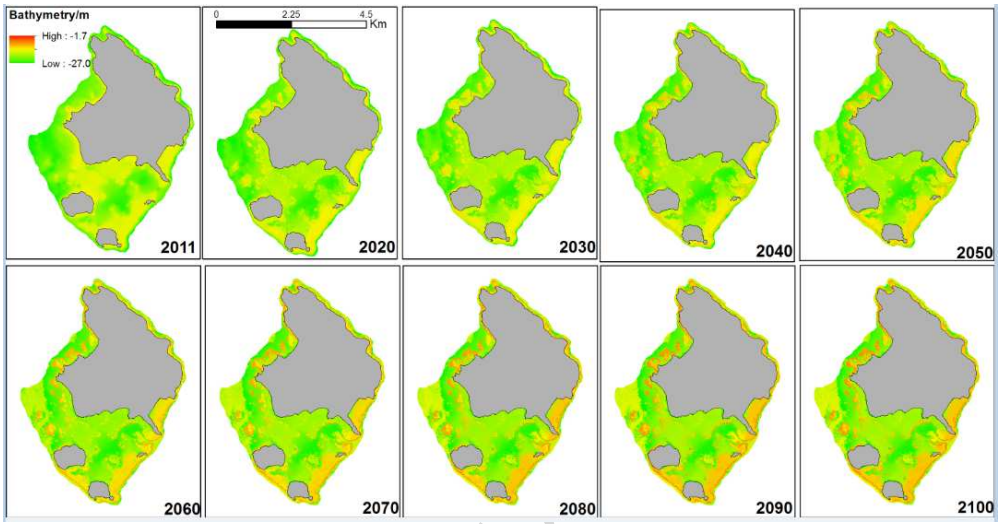

Figure 4

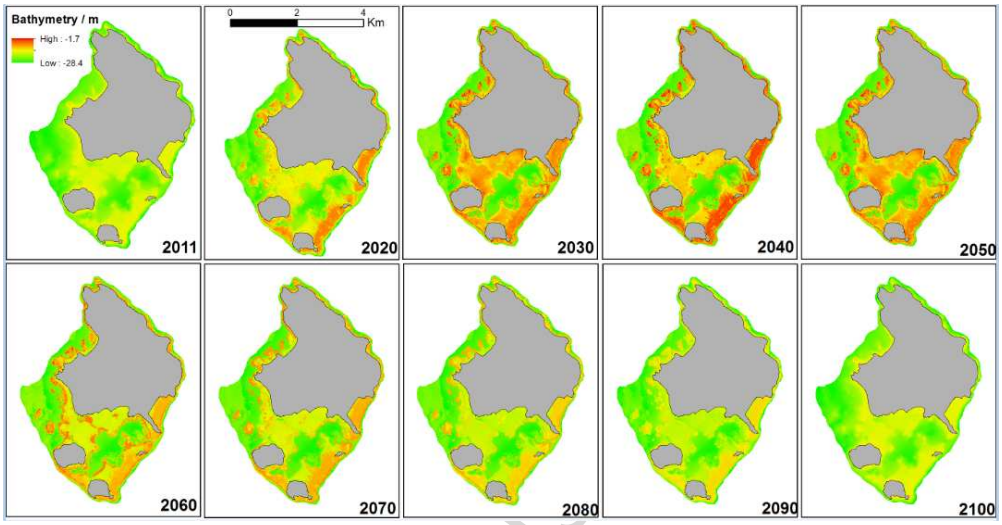

Figure 5

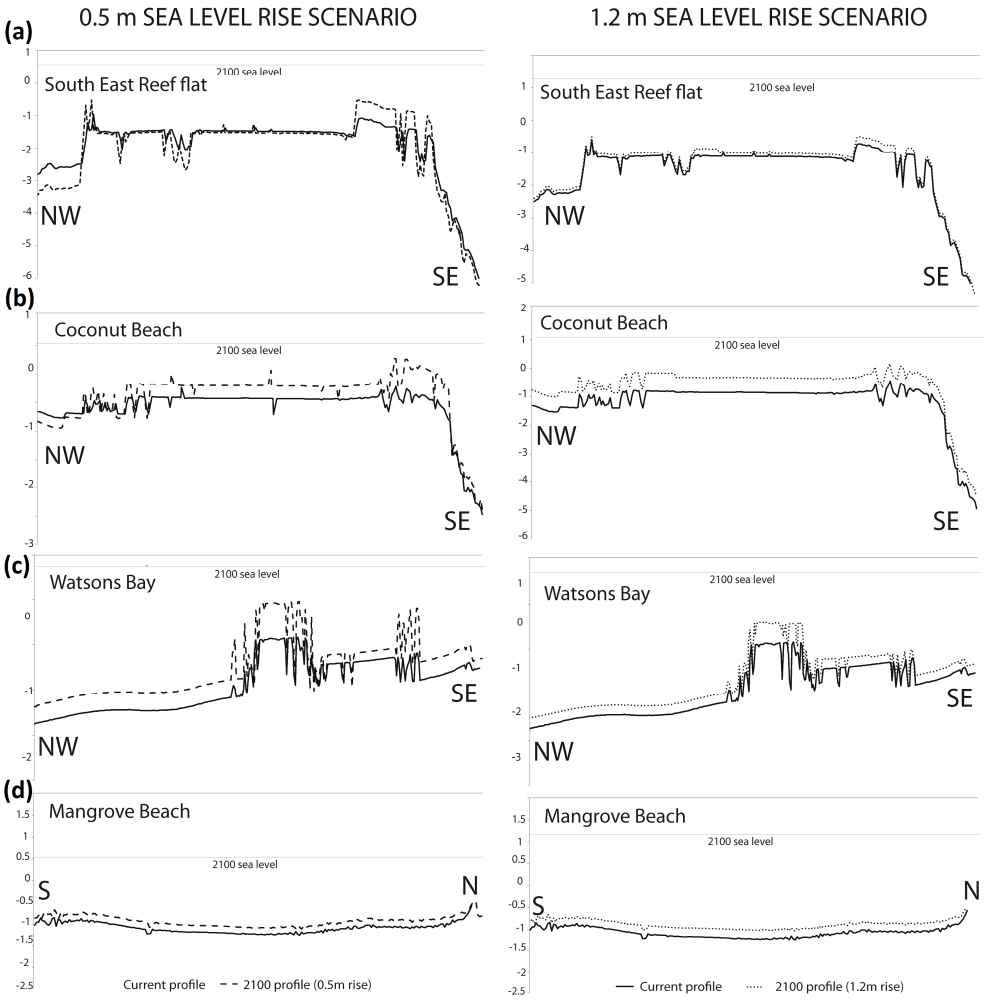

Figure 6

Table 1. Published values for calcification rates for the different reef environments around Lizard Island.

Environment	Calcification rate ($kg\ m^{-2}\ yr^{-1}$)	Reference
Seaward reef flat		
- (Transect A)	3.47 – 3.83	LIMER, 1975
Lagoon entrance channel coral pinnacle		
-(Site P: Pinnacle at lagoon entrance)	3.65	
Central to leeward reef flat		
-(Transect D: Across western lagoonal reef flat)	4.56	
Zone D1 (inner reef flat)	3.10	
Zone D2 (middle reef flat)	0.91	
Zone D3 (outer reef flat)		
Shallow, seaward reef flat		Smith and Kinsey, 1976
Algal pavement	3.8	
Coral-algal cover	3.6	
Top of coral pinnacle	3.7	
Protected environment		
Lagoon	1	
Benthic Foraminifer, reef flat		Smith and Wiebe, 1977
Marginopora vertebralis	0.78	
Windward calcified algae	1.5 – 10.3	Chisholm, 2000

Table 2. Census-based measures of annual carbonate gain and reef accretion for biotic components of the Lizard Island reef system (*G parameterised using values from studies in Table 1, with additional values taken where necessary from Harney and Fletcher 2003, Vescei, 2004 and Hart and Kench 2007. n= number of video footage samples). The accretion rate of 6.7 mm yr^{-1} exceeds observational data as it relates to the productive forereef habitat, where carbonate gains cannot be measured using hydrochemical methods because of open water mixing.

Map class	**n**	**Biotic assemblage (Average % cover)**	**Map class rate of production/ kg m^{-2} yr^{-1}**	**Map class rate of reef accretion mm yr^{-1}**
1. Coral	35	Live coral (90%) Soft coral (5%) Calcified macroalgae (5%)	10.45	6.70
2. Coral, soft coral and calcified algae on reef flat	57	Digitate and tabulate *Acropora* (20%) Encrusting coral (15%) Encrusting calcified algae (15%) Soft coral (10%) Dead coral framework (15%) Sand (12%) Rubble (3%)	6.14	4.06
3. Calcified algae with sparse coral	23	Live coral (30%) Dead coral (30%) Calcified macroalgae (15%) Soft coral (10%) Algae (10%) Sand (5%)	5.80	3.90
4. Algae and rubble on sand	52	Sand (90%) Algae (4%) Rubble (6%)	5.48	3.53
5. Dead coral framework	23	Dead coral (45%) Turf algae (50%) Rubble (5%)	2.50	2.01
6. High density seagrass	18	Seagrass (80%) Sand (20%)	2.44	1.98
7. Sparse coral, rubble and algae on sand	34	Sand (80%) Dead coral (5%) Live coral (5%) Rubble (5%) Algae (5%)	1.70	0.92
8. Low density algae on sand	57	Sand (85%) Algae (15%)	1.30	0.72
9. Low density seagrass	19	Sand (85%) Seagrass (15%)	1.27	1.02
10. Sand	46	Bare carbonate sand (100%)	1.00	0.93